

## DISPERSION STRENGTHENED Al – Al<sub>4</sub>C<sub>3</sub> MATERIAL PREPARED BY MECHANICAL ALLOYING

M. Besterčí, G. Jangg, M. Šlesár, J. Zrník

### ABSTRACT

*Dispersion strengthened aluminium compacts have been prepared by powder metallurgy. The base microstructure is an aluminium matrix strengthened with dispersed ceramic particles. The strengthening is direct through dislocation movement retardation, and indirect through deformation induced by microstructure modification in the next technological steps. The method of mechanical alloying process is described. Carbon transformation to carbide Al<sub>4</sub>C<sub>3</sub> is characterised within different heat treatment schedules and nine commercial carbon powders tested. The micromechanism of carbon incorporation into the metallic powder, and the compacting of it are described. The influence of dispersed carbides on mechanical properties is evaluated together with the influence of deformation on microstructure and properties. Ductility anomalies up to the type of superplasticity, were observed at certain tensile testing strain rates. The high temperature tensile test, resistance to creep, and creep-fatigue test results are available.*

**Keywords:** *aluminium-graphite powder system, mechanical alloying, carbon to Al<sub>4</sub>C<sub>3</sub> transformation, Al-Al<sub>4</sub>C<sub>3</sub> dispersion strengthening system, microstructure, tensile deformation, strain rate, superplasticity, creep, creep - fatigue behaviour*

### INTRODUCTION

An advance in properties is sought for all materials including materials prepared by the technology of powder metallurgy. There are different ways to prepare the system matrix-dispersoid [1]. With the advent of mechanical alloying, it became possible to put the theoretical concept into practice by incorporating very fine particles, in a fairly uniform distribution, into a metal matrix. The mechanical alloying was first developed and used to prepare immiscible alloys and superalloys with a nickel matrix, and the method spread to other alloys later. The process starts with dry, high energy milling of the matrix powder with dispersoid, producing a homogeneous composite with a fine controlled microstructure. The intense milling is resulting in matrix with even distribution of dispersed particles. Dispersoids can be formed in a solid state reaction by introducing materials that react with the matrix in the time following heat treatment, [2].

A mode of mechanical alloying is reaction milling, developed for dispersion strengthened aluminium production [3, 4]. To produce aluminium dispersoid the aluminium powder is intensively dry milled with carbon powder. The transformed dispersed phase Al<sub>4</sub>C<sub>3</sub> is than produced by a chemical reaction, which starts during milling, and it is

completed at the next heat treatment process. The resulting powder mixture is then pressed, compacted and the compacts are prepared by isostatic pressing and hot extrusion.

The aim of this paper is to study the influence of the various graphite types when mixed with Al powder, and heat treatment procedure on the microstructure and properties of dispersion strengthened aluminium type Al-Al<sub>4</sub>C<sub>3</sub>. The influence of carbides characteristics on mechanical properties is evaluated together with the influence of applied deformation mode on the microstructure development and mechanical properties.

## EXPERIMENTAL MATERIAL AND METHODS

The experimental material - dispersion strengthened aluminium with Al<sub>4</sub>C<sub>3</sub> particles, was prepared by intense milling of aluminium powder with different types of carbon, as shown in Tab.1. The prime aluminium powder grain size was 100 µm with the carbon content of 0.6 - 3 wt. %.

The aluminium composite dispersion strengthened by Al<sub>4</sub>C<sub>3</sub> particles, has been prepared by the method of mechanical alloying. The final carbide content was in the range of 2.5 - 12 vol.%. The obtained mixture was compacted at 600 MPa and thermally treated at 450, 500, 550, and 600°C whereas treatment times of 1, 3, 10, and 30 hours were employed. The final compacting by hot extrusion at a temperature of 550°C and a reduction rate of 94% on the cross section was applied [5]. The experimental material has been both prepared, and tested by gas chromatography for carbides Al<sub>4</sub>C<sub>3</sub> content, at the Institute for Chemical Technology of Inorganic Materials, TU Vienna.

Tab.1. Types of different carbon types used

Notation	Type	Commercial Carbon	Notation	Type	Commercial Carbon
A	a <sub>1</sub>	LTD	F	a <sub>2</sub>	Farbruss FW 2
B	a <sub>1</sub>	Spezialschwarz 5	G	a <sub>2</sub>	Flammruss 101
C	a <sub>1</sub>	Spezialschwarz 500	H	c	Thermax
D	a <sub>1</sub>	Printex 30	I	b	Grafit KS 2,5
E	a <sub>2</sub>	Printex 400			

## MILLING AND CARBONIZATION KINETICS

For the nine employed types of commercial carbon system Al – 8Al<sub>4</sub>C<sub>3</sub> labelled A to I, correlations were sought between the physical and chemical properties and milling parameters, or carbide transformation rate, and properties of the produced compacts.

The different carbon types showed different distributions of carbon in the aluminium powder. Their susceptibility to milling was measured by the ability to prepare homogeneous distribution without clusters being formed. According to the obtained results the carbon forms were divided into 4 types:

a<sub>1</sub>) porous types of furnace black, made by the incomplete burning of carbohydrates at low temperatures, with very good properties. They are fine, with high contact surface, and an easy destruction of clusters.

a<sub>2</sub>) porous types of furnace black, made by the incomplete burning of carbohydrates at higher temperatures. They are fine, but they form more stable clusters, resistant to disintegration.

b) electrographite, with a layered structure, with good susceptibility to milling, though coarse grained and with a smaller contact surface; comparable to furnace black (a<sub>1</sub>, and a<sub>2</sub>)

c) cracked carbon, forms strong clusters, and the carbon to carbide transformation rate is low.

The milling kinetics of the system is described in more detail in reference [6]. From the results, the homogeneity of carbide distribution and contact surface area influence the Al+C transformation kinetics to  $Al_4C_3$ . The dependence of the transformation rate on temperature and hold time for the 4 carbon types is shown in Fig.1. The good susceptibility to transformation for porous furnace black ( $a_1$  and  $a_2$ ) and that of electrographite (b) is evident.

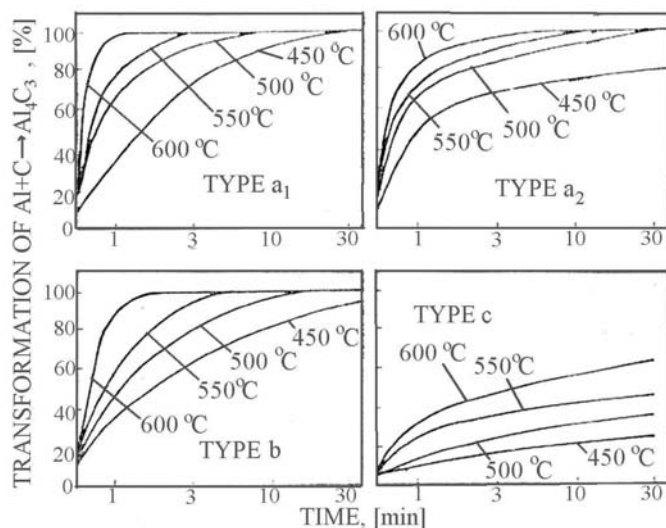


Fig.1. Dependence of carbon to the carbide transformation rate on heat treatment temperature and hold time for four carbon types.

The porous carbon types are incorporated into the matrix by friction during milling, the distribution is even, and clustering is small. On the other side, hard graphite (c), resists disintegration and the granules are large as documented in Fig.2. The dependence of macro, and microhardness on carbon to carbide transition is shown in Fig.3.

The percentage of carbon transformed to carbide  $Al_4C_3$  is defined as the Quality factor (QF) and it expresses the measure of the dispersion technology efficiency. For different types of heat treatment, it is shown in Tab.2. The QF was used in [7] for empirical correlation calculations of the dependence of strengthening on dispersed phase content. The correlation was expressed by relation

$$\frac{Rm + 500}{1420} (A_5)^{0.219} = QF \quad (1)$$

where Rm is tensile strength and  $A_5$  is elongation.

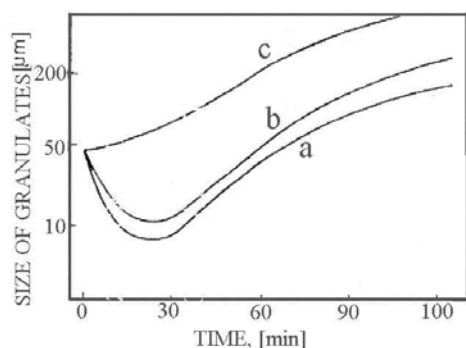


Fig.2. Mean grain size dependence on milling time and carbon type a), b), c) for  $\text{Al} - 4\text{Al}_4\text{C}_3$ .

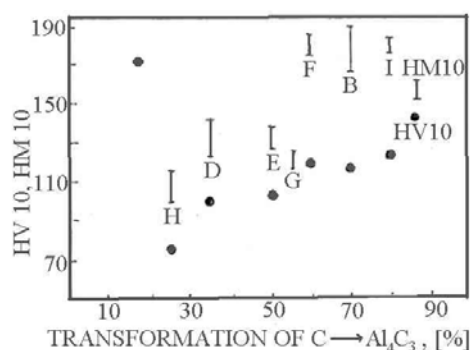


Fig.3. Dependence of macro and micro hardness on carbon to carbon transition

The maximum value of QF is equal to 1, and this value corresponds to the total transformation of carbon to carbide  $\text{Al}_4\text{C}_3$ . This value classifies the quality of both milling and transformation heat treatment processes together. The QF values of the investigated systems are presented in Tab.2.

Tab.2. Dispersion technology efficiency, the portion of carbon transformed to  $\text{Al}_4\text{C}_3$ , with heat treatment and Quality factor.

Heat treatment: 450°C/ 30 h					Heat treatment: 600°C/ 30 h				
Notation	Commercial mark	% $\text{C} \rightarrow \text{Al}_4\text{C}_3$	Vol.% $\text{Al}_4\text{C}_3$	QF	Notation	Commercial mark	% $\text{C} \rightarrow \text{Al}_4\text{C}_3$	Vol.% $\text{Al}_4\text{C}_3$	QF
A	LTD	100	12.6	0.85	A	LTD	100	12.6	1.00
I	KS 2.5	78	9.8	0.75	I	KS 2.5	100	12.6	0.95
C	Spezialschwarz 550	76	9.6	0.82	C	Spezialschwarz 550	100	12.6	1.00
B	Spezialschwarz 5	68	8.6	0.86	B	Spezialschwarz 5	100	12.6	1.00
F	Farbruss FW 2	58	7.3	0.87	F	Farbruss FW 2	100	12.6	1.00
G	Flammruss 101	55	6.9	0.81	G	Flammruss 101	98	12.3	0.91
E	Printex 400	50	6.3	0.80	E	Printex 400	94	11.8	0.99
D	Printex 30	36	4.5	0.85	D	Printex 30	92	11.6	1.00
H	Thermax	25	3.2	0.80	H	Thermax	64	8.1	0.92

The dependence of tensile strength and ductility on carbon content (wt.%) for Flammruss LTD is presented in Fig.4. The temperature dependence of tensile strength for various carbon contents (wt. %) is documented in Fig.5.

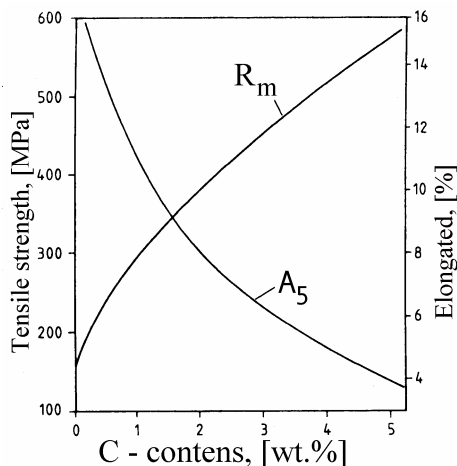


Fig. 4. The dependence of tensile strength and ductility on carbon content (wt.%) for Flamms LTD

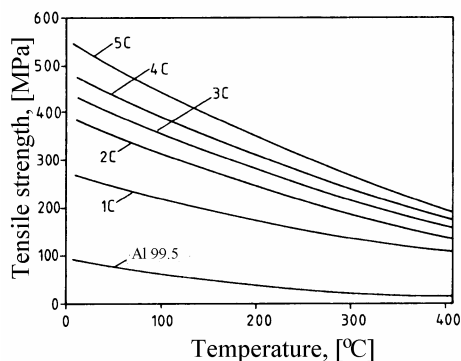


Fig. 5. The temperature dependence of tensile strength for various carbon contents.

## MICROSTRUCTURE AND MECHANICAL PROPERTIES

Light microscopy microstructure analysis of the produced compacts proved a high homogeneity of dispersed particle distribution in the direction perpendicular to the direction of hot extrusion. In the longitudinal direction of the bar as a result of hot extrusion the  $\text{Al}_4\text{C}_3$  carbide particles were arranged into bands. Impurities like  $\text{Al}_2\text{O}_3$  and  $\text{FeAl}_3$  particles were found in the structure. Residual, quite large carbon particles were observed after heat treatment at  $450^\circ\text{C}$  for 30 hours. The distance between the bands was found to be different. The matrix grain boundaries were not observable.

Electron microscopy analysis was conducted using carbon replicas and thin foils. The carbon replicas were not of help for quantitative evaluation. Transmission electron microscopy of thin foils offered better results. For all the tested carbon combinations from the A to I labels, thin foils were produced for the heat treatment  $450^\circ\text{C}/30$  h. The  $\text{Al}_4\text{C}_3$  particle size and the subgrain size were measured using the thin foils. The dispersed phase  $\text{Al}_4\text{C}_3$  particle size was measured on 200 to 300 thin foil structures, and it was constant and as small as 30 nm. The particle size was not influenced neither by the carbon type nor by the heat treatment technology applied.

The mean distance between the particles  $\lambda$  was calculated according the equation:

$$\lambda = \frac{2d_0}{3f(1-f)} \quad (2)$$

where  $d_0$  is the mean particle size,  $f$  is the volume fraction of dispersed particles.

The mean distance between the particles depended strongly on the carbon type, as it depends on the efficiency of transformation. Subgrain size measured in the range of 100 grains in thin foils depended on the carbon type, as well. It ranged from 0.3 to  $0.7 \mu\text{m}$ . The stability of properties, resulting from graphite type I (KS 2.5), led to the highest production and utilization of this type of dispersion strengthening. The results on mechanical behaviour of the compacted system, listed in the next parts of this paper are for this material selected.

In our previous works [8, 9, 10], we have evaluated the distance between the particles by point object simulation methods. The example of four interparticle distance categories are shown in Fig.6. This includes the mean interparticle distance  $\lambda_\mu$ , the mean minimum distance  $\lambda_p$ , the mean visibility  $\lambda_v$ , and the mean free spherical contact distance  $\lambda_g$ . The characteristics and properties of these parameters have been analyzed in [9].

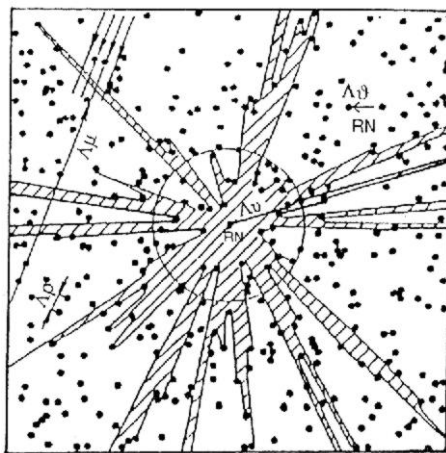


Fig.6. Interparticle distance categories

During the last years, a new approach to the description of point systems has been developed intensively, which is referred to as polygonal methods [1]. The dual representation formed in the above way describes completely the given point system. Properties of Voronoi tessellation and their various generalizations are being very intensively studied now, the state of this study is given in the monograph [11]. Intermediate stages of evaluation for this foil (a), outlines of particles (b), and of reference points (c) are documented in Fig.7.

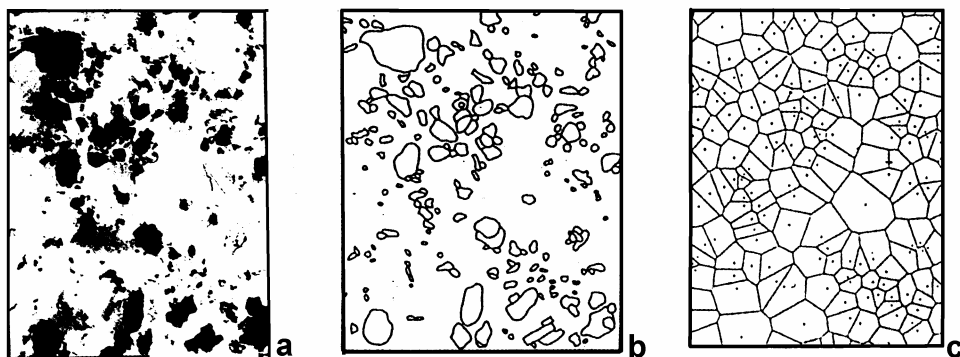


Fig.7. Intermediate stages of evaluation for this foil (a), outlines of particles (b) and reference points (c)

Mechanical properties and microstructure of dispersoid, dependant on the volume content of the dispersed phase  $\text{Al}_4\text{C}_3$ , as shown in Fig.8 (450°C/30 h), are influenced by the

technology applied. With the near-constant dispersed particle grain size, the influence on strength and plasticity corresponds to the subgrain size and the mean dispersed interparticle distance. The effect of a low temperature of the heat treatment on carbide reaction, revealed more differences in structural parameters, tensile strength and elongation. From the point of a strength increase, the carbon types A, C, and I showed the best results. Increasing the transformed carbon content, and increasing the volume content of the dispersed phase in the aluminium matrix, the tensile strength increased and plastic properties decreased as interparticle distance  $\lambda$  decreases.

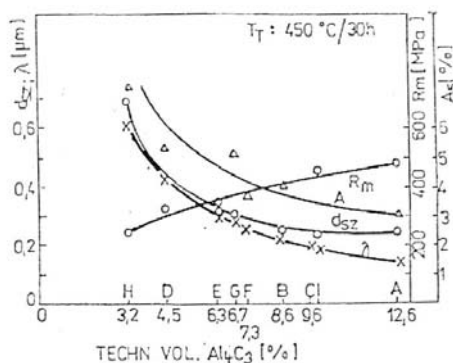


Fig.8. Mechanical properties and microstructure parameters in dependence on  $\text{Al}_4\text{C}_3$  content

The data from Tab.2 and the results from calculations of the interparticle distance, revealed that the carbon type used in the mixing technology, i.e. by its susceptibility to milling and chemical reaction, controls the microstructure of the dispersoid. The representative substructures related to process condition are documented in Fig.9 and Fig.10. The subgrain size can be another measure of microstructure control in the investigated material.

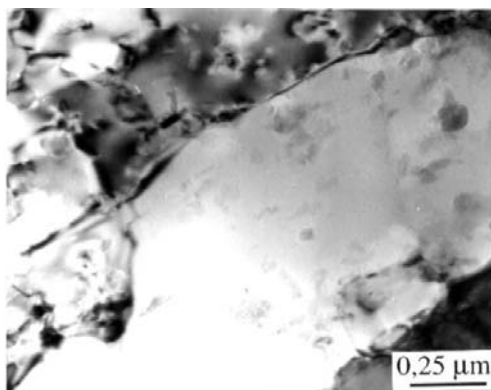


Fig.9. TEM micrograph of Al - $\text{Al}_4\text{C}_3$  with 3 wt. % carbon type I.

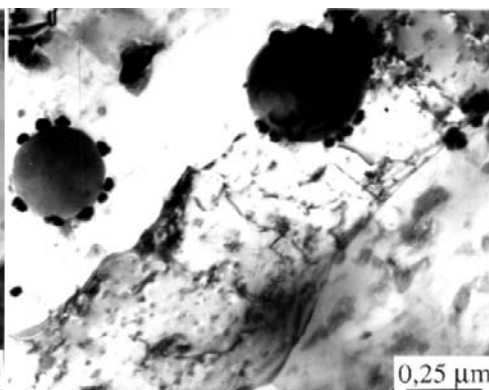


Fig.10. TEM micrograph of Al - $\text{Al}_4\text{C}_3$  with 3 wt. % carbon type H

Low strengthening was found for materials with carbon of type H, which corresponds to low carbon transformation efficiency and low phase  $\text{Al}_4\text{C}_3$  volume content.



The substructure obtained with carbon type H is illustrated in Fig.10. Materials with carbon types B, F, G, and E, belong to the mid-point group by influence on mechanical properties. The corresponding quality factor QF, is the result of carbide distribution and subsequent strengthening effect.

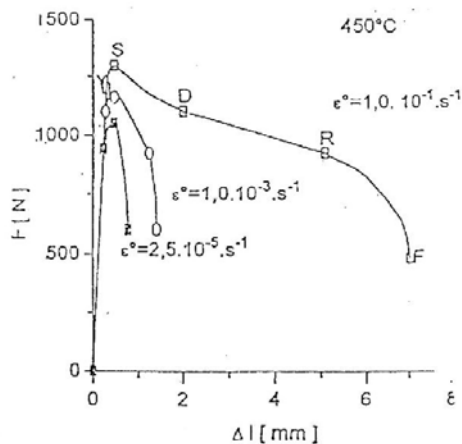


Fig.11. Stress-strain dependences at 450°C.

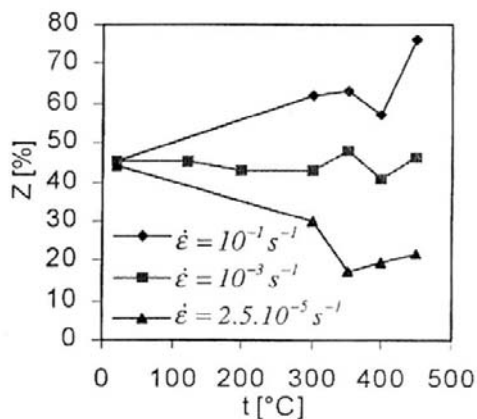


Fig.12. Reduction of area Z as a function of strain rate and temperature.

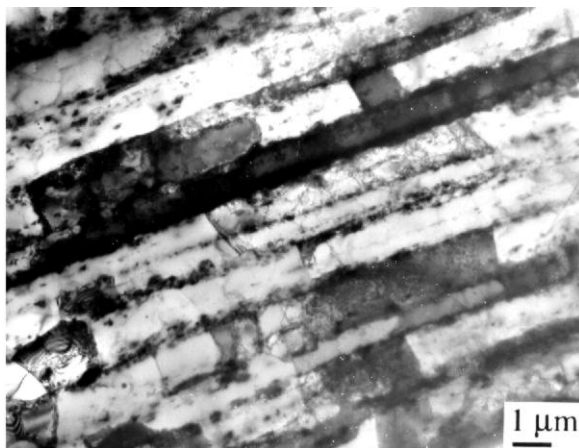


Fig.13. TEM micrograph of recovered substructure with elongated grains of Al - 4Al<sub>4</sub>C<sub>3</sub> material

The Al-Al<sub>4</sub>C<sub>3</sub> system with 4 vol. % of Al<sub>4</sub>C<sub>3</sub> was tested under different tensile conditions, where three different strain rates and different testing temperatures up to 450°C were used [12]. The results are shown in Fig.11. The deformation mechanism and fracture mechanism were analysed corresponding to different testing conditions. For the higher strain rates of 10<sup>-1</sup> s<sup>-1</sup> at 450°C, a significant growth of plastic properties was observed. The high uniform elongation A<sub>5</sub> of the specimen gauge length, and corresponding reduction values of the reduction in area Z were manifested in Fig.12. The ductility anomalies are showing an onset of a type of superplasticity. The recovered substructure, which resulted



due to testing conditions, is documented in Fig.13. On the other hand, when testing temperature was of  $450^{\circ}\text{C}$  and low strain rates  $10^{-5} \text{ s}^{-1}$ , the microstructure was polygonized. Sliding along grain boundaries, accommodated by dislocation creep, would be the prevailing mechanism of deformation and plastic properties are extremely low. According to [16] it was proved that for materials Al -  $12\text{Al}_4\text{C}_3$ , the main mechanism responsible for superplastic behaviour is the grains rotation process and not sliding. As an evidence of this process, one may use the result on grain size and measurement shape control at longitudinal and transverse direction carried out in thin foils. The mechanisms of grain re-arrangement in superplasticity deformation process by sliding (a) and by rotation (b) are documented on Fig.14. The fracture mechanism was dominantly intergranular.

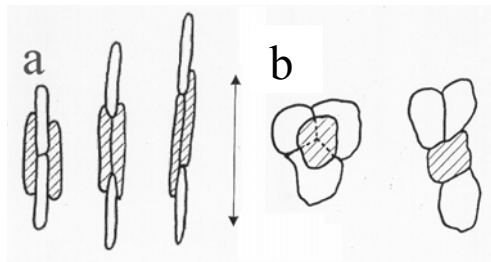


Fig.14. The mechanisms of grain re-arrangement in superplasticity deformation process by sliding (a) and by rotation (b)

The creep properties of dispersion strengthened Al -  $2.5\text{Al}_4\text{C}_3$  dispersoid and Al- $10\text{Al}_4\text{C}_3$  dispersoid were tested at  $350$  to  $450^{\circ}\text{C}$ , and testing conditions and detailed results are discussed in [13] and [14]. The creep results are presented in Fig.15. The creep is controlled by lattice diffusion. The creep mechanism was explained taking for the start point the Ansell-Weertman model.

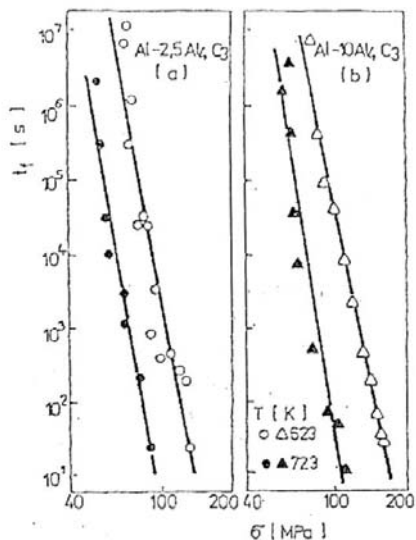


Fig.15. Dependence of applied creep stress at various temperatures.

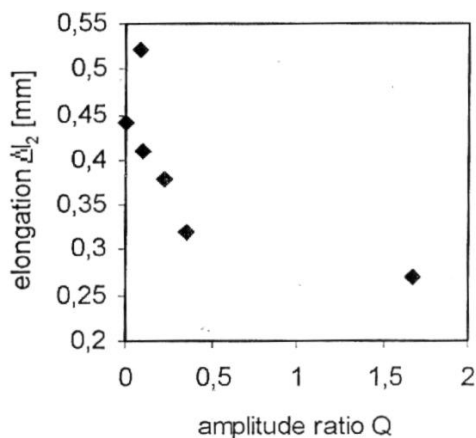


Fig.16. Dependence of elongation on amplitude ratio at cyclic creep

The creep-fatigue deformation behaviour of Al-8Al<sub>4</sub>C<sub>3</sub> dispersoid system was analysed at 400°C as well [15]. The introduction of the cyclic stress component of various cyclic amplitude  $\sigma_A$  onto the creep mean stress of  $\sigma_{max}$  showed specific influence on the lifetime of tested specimens. There was a definite increase on the time to fracture in cases of the smaller stress ratio R and for higher applied frequencies. The dependence of the strain, expressed by a specimen's elongation against amplitude ratio Q for different cyclic frequency, is shown in Fig.16. By comparing the results with those for pure creep, the introduction of the cyclic stress component irregularly influenced the strain to fracture and resulted in a scattering of life time values depending on amplitude ratio Q and cyclic frequency.

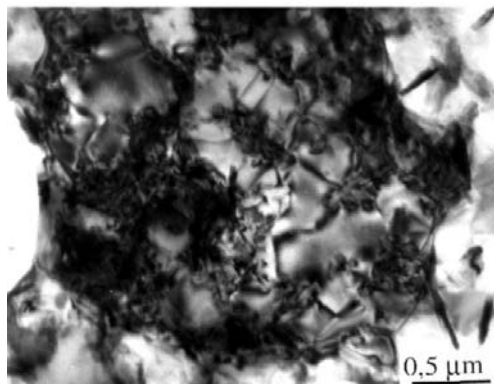


Fig.17. TEM micrograph showing creep - deformed substructure of Al - 8Al<sub>4</sub>C<sub>3</sub> material

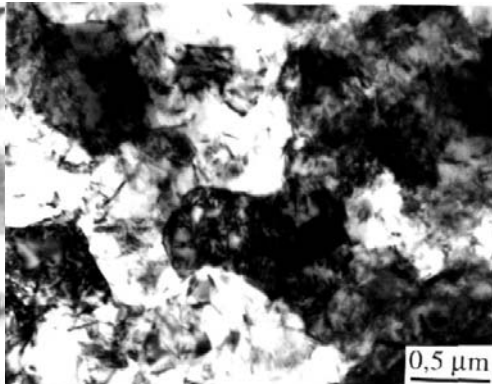


Fig.18. TEM micrograph showing cyclically deformed substructure of Al - 8Al<sub>4</sub>C<sub>3</sub> material

The analysis of the deformation mechanism by evaluation of the substructure, has confirmed the onset of polygonization process during creep, Fig.17. The cyclic stress component, regardless of the frequency or stress ranges, was reflected in the formation of a dislocation substructure similar to that of pure creep, Fig.18. Considering the fracture mechanism, corresponding to all cyclic creep tests it did not show any particular influence on fracture morphology, which might have participated either at the crack nucleation or in the time of crack propagation. Fractures were prevailingly intergranular, showing no influence of the presence of a fatigue stress component on fracture mechanism.

## CONCLUSIONS

The obtained results on the mechanical alloying process and heat treatment of Al - C system, and on deformation behaviour of dispersion strengthened Al - Al<sub>4</sub>C<sub>3</sub> system prepared under different conditions, can be summarized as follows:

- It was shown that the transformation efficiency of carbon to Al<sub>4</sub>C<sub>3</sub> by heat treatment of aluminium with the porous furnace black a) and electrographite b) is higher, than that of the hard cracked graphite c).
- The volume fraction of carbide phase Al<sub>4</sub>C<sub>3</sub> and the efficiency of transformation, are in good agreement with resulting microstructure and achieved mechanical properties.
- The quality factor QF is a good evaluation tool of the milling process and of heat treatment produced transformation.

- Microstructure and mechanical properties showed that the best strengthening is obtained with carbon types LTD (A) and KS 2,5 (I) with a high transformation rate, high  $\text{Al}_4\text{C}_3$  carbide content, and low subgrain size. On the other side, the strengthening resulted from the cracked Thermax (H) graphite is the lowest due to the low transformation rate  $\text{Al} + \text{C} \rightarrow \text{Al}_4\text{C}_3$
- The stability of properties obtained with graphite type I (KS 2,5), leads to the highest production and utilization of this type of dispersion strengthening.
- The temperature dependencies of ductility, and reduction of area in temperature range of 350–450°C and strain rate of  $10^{-1} \text{ s}^{-1}$ , indicated a considerable increase of these properties. In a case when the volume fraction of  $\text{Al}_4\text{C}_3$  changes from lower to higher, the grain rotation mechanism dominates instead of the grain boundary sliding.
- The creep mechanism is controlled by lattice diffusion.
- The introduction of the cyclic creep stress component onto constant creep stress, has shown an influence on the fracture life of the dispersoid in dependence on cyclic frequency and stress ratio Q. The microstructure study proved that recovery process accompanied deformation process during creep and cyclic creep as well.

## REFERENCES

- [1] Besterčí, M.: Dispersion strengthened Al prepared by mechanical alloying. Cambridge : Int.Science Publ, 1999. ISBN 189832655
- [2] Weissgäerber, T., Kieback, B.: Materials Science Forum, vol. 8, 2000, p. 275.
- [3] Korb, G., Jangg, G., Kutner, F.: Draht, vol. 30, 1975, p. 318.
- [4] Jangg, G., Kutner, F., Korb, G.: Aluminium, vol. 51, 1975, p. 641 Publ, 1999, ISBN 189832655.
- [5] Besterčí, M., Šlesár, M., Jangg, G., Miškovičová, M., Ďurišin, J.: Kovové materiály, vol. 27, 1989, no. 1, p. 77.
- [6] Jangg, G., Šlesár, M., Besterčí, M., Zbiral, J.: Zeischrift f. Werkstofftechnik, vol. 20, 1989, p. 226.
- [7] Jangg, G., Vasgyura, J., Schröder, K., Šlesár, M., Besterčí, M. In: Inter. Conf. Powder Metallurgy and Exh. Düsseldorf, 1986, p. 989.
- [8] Saxl, I., Besterčí, M., Pelikán, K.: Pokroky práškové metalurgie, vol. 3, 1986, no. 4.
- [9] Saxl, I., Pelikán, K., Rataj, J., Besterčí, M.: Quantification and Modelling of Heterogenous Systems. Cambridge Int. Publication, 1995. ISBN 1898326045
- [10] Besterčí, M., Kohútek, I., Saxl, I., Sülleiová, K.: Journal of Materials Science, vol 34, 1999, p. 1055.
- [11] Okabe, A., Boots, B., Sugihara, K.: Spatial Tessellation. Chichester : J. Wiley, 1992
- [12] Besterčí, M., Zrník, J., Šlesár, M.: Kovové materiály, vol. 35, 1997, no. 5, p. 344.
- [13] Orlová, A., Kuchářová, K., Čadek, J., Besterčí, M.: Kovové materiály, vol. 35, 1986, p. 505.
- [14] Besterčí, M., Čadek, J.: Pokroky práškové metalurgie, vol. 3, 1993, p. 17.
- [15] Zrník, J., Besterčí, M., Kováč, L., Horňák, P.: Proc. ICAA5 Alum. Alloys, Grenoble, France, 1996.
- [16] Besterčí, M., Velgosová, O., Ivan, J., Kováč, L.: Kovové materiály, vol. 39, 2001, no. 5, p. 309.